SIAM J. SCI. COMPUT.
Vol. 42, No. 4, pp. A2325–A2343

IDENTIFICATION OF POINT-LIKE OBJECTS WITH MULTIFREQUENCY SPARSE DATA*

XIA JI† AND XIAODONG LIU‡

Abstract. The inverse acoustic scattering of point objects using multifrequency sparse measurements is studied. The objects may be a sum of point sources or point-like scatterers. We show that the locations and scattering strengths of the point objects can be uniquely identified by the multifrequency near or far fields taken at sparse sensors. Based on the uniqueness analysis, some direct methods have also been proposed for reconstructing the locations and determining the scattering strengths. The numerical examples are conducted to show the validity and robustness of the proposed numerical methods.

Key words. inverse scattering, multifrequency, sparse data, uniqueness, sampling method

AMS subject classifications. 35P25, 45Q05, 78A46, 74B05

DOI. 10.1137/20M1312551

1. Introduction.

The inverse scattering theory aims to reconstruct the unknown objects from the wave measurements. This plays an important role in many areas such as radar, nondestructive testing, medical imaging, geophysical prospection, and remote sensing. We refer the reader to the standard monograph [3] for a research statement on the significant progress in both the mathematical theories and the numerical approaches.

A practical difficulty is when measurements are difficult or even impossible to be taken completely around the unknown objects. Actually, the measurements are often available from a few sensors (i.e., a sparse array). At a fixed sensor, it is easy to vary frequency to obtain more data. This is still a small set of data, which indeed brings many difficulties for the solvability of the inverse problems. The first result was given in 2005 by Sylvester and Kelly [13], where they considered the linear inverse acoustic source problems and showed that a convex polygon containing the unknown source with normals in the observation directions can be uniquely determined by the multifrequency sparse far field patterns. This implies, even for such a small data set, that one can make a meaningful statement about the size and location of the source. A factorization method using sparse multifrequency far field measurements was recently introduced in [7] to produce a union of convex polygons that approximate the locations and the geometry of well-separated source components. We also refer the reader to [1], where a direct sampling method using sparse multifrequency far field measurements is designed to reconstruct the location and shape. Surprisingly, even the concave part of the source support can be well reconstructed with enough observation directions. However, the corresponding theoretical basis is still not established. Such a direct

*Submitted to the journal's Methods and Algorithms for Scientific Computing section January 13, 2020; accepted for publication (in revised form) May 7, 2020; published electronically August 4, 2020.

https://doi.org/10.1137/20M1312551

Funding: The work of the first author was supported by the NSFC through grants 91630313 and 11971468. The work of the second author was supported by the NSFC through grant 11971471 and by the CAS Youth Innovation Promotion.

†School of Mathematics and Statistics, and Beijing Key Laboratory on MCAACI, Beijing Institute of Technology, Beijing, 100081, China (jixia@lsec.cc.ac.cn).

‡NCMIS and Academy of Mathematics and Systems Science, Chinese Academy of Sciences, Beijing, 100190, China (xdliu@amt.ac.cn).

sampling method was recently generalized for inverse acoustic, elastic, and electromagnetic source scattering problems with phased or phaseless multifrequency sparse far field data [9, 10, 11]. It was also shown in [1] that the smallest annular centered at the sensor containing the source support in $\mathbb{R}^3$ can be uniquely determined by the multifrequency scattered fields taken at the sensor. Difficulties arise for the inverse obstacle/medium scattering problems because these problems are nonlinear. Sylvester and Kelly [13] considered Born approximation to the inverse medium problem and obtained similar results as for the inverse source problem. The MUSIC (MUltiple SIgnal Classification) algorithm [6] is studied for locating small inhomogeneities. Based on the weak scattering approximation and the Kirchhoff approximation, a direct sampling method is proposed for location and shape reconstruction of the underlying objects [8] by using multifrequency sparse backscattering far field measurements.

In practical radar and remote sensing, faraway objects radiate fields that, within measurement precision, are nearly those radiated by point-like objects. The objects may be a sum of point sources or point-like scatterers. Most of the works focus on locating the positions, e.g., MUSIC [2, 4, 12] for point-like scatterers and the direct sampling method [14] for point sources. This paper aims not only to locate the positions, but also to recover the scattering strengths based on the multifrequency sparse near or far fields. In the recent manuscript [8], the point-like obstacles were considered with multifrequency sparse backscattering far field patterns. We clarify the smallest number of sensors and frequencies to be used in this paper by following the idea from [6]. Furthermore, we show the uniqueness of the scattering strengths and introduce the corresponding formula. Inspired by the idea in the phase retrieval algorithm proposed in [9, 10, 11], we introduce a simple numerical algorithm for identifying one point with a few scattered fields or far fields. Based on the uniqueness analyses, some novel direct methods are also designed to locate the multiple points and to reconstruct the scattering strengths.

The remaining part of the work is organized as follows. In the next section, we introduce the inverse scattering of point sources and the inverse scattering of plane waves by point like scatterers. We then proceed in section 3 for the uniqueness results with sparse data. Section 4 is devoted to some numerical methods for reconstructing the locations and scattering strengths of the point objects. The numerical methods are then verified in section 5 by extensive examples.

2. Scattering by point objects. We begin with the formulations of the acoustic scattering problem. Let $k = \omega/c > 0$ be the wave number of a time harmonic wave, where $\omega > 0$ and $c > 0$ denote the frequency and sound speed, respectively. In the whole paper, we consider multiple frequencies in a bounded band, i.e.,

$$k \in (k_-, k^+), \tag{2.1}$$

with two positive wave numbers k_- and k^+. Recall the fundamental solution $\Phi_k(x, y)$, $x, y \in \mathbb{R}^n, x \neq y$, of the Helmholtz equation, which is given by

$$\Phi_k(x,y) := \begin{cases} \dfrac{ik}{4\pi} h_0^{(1)}(k|x-y|) = \dfrac{e^{ik|x-y|}}{4\pi|x-y|}, & n = 3, \\ \dfrac{i}{4} H_0^{(1)}(k|x-y|), & n = 2. \end{cases} \tag{2.2}$$

Here, $h_0^{(1)}$ and $H_0^{(1)}$ are, respectively, the spherical Hankel function and Hankel function of the first kind and order zero.

Point sources. We consider an array of M point sources located at $z_1, z_2, \ldots, z_M \in \mathbb{R}^n$ in the homogeneous space $\mathbb{R}^n, n = 2, 3$, and denote by $\tau_m \in \mathbb{C}\backslash\{0\}$ the scattering strength of the mth point source. The scattered field u^s is a solution of the equation

$$\Delta u^s + k^2 u^s = \sum_{m=1}^{M} \tau_m \delta_{z_m} \quad \text{in } \mathbb{R}^n,$$

with δ_{z_m} denoting the Dirac measure on $\mathbb{R}^n$ giving unit mass to the point z_m, $m = 1, 2, \ldots, M$. Precisely, the scattered field u^s is given by

$$u^s(x,k) = \sum_{m=1}^{M} \tau_m \Phi_k(x, z_m), \quad x \in \mathbb{R}^n\backslash\{z_1, z_2, \ldots, z_M\}. \tag{2.3}$$

From the asymptotic behavior of $\Phi_k(x,y)$, we conclude that

(2.4)
$$u^s(x,k) = \frac{e^{i\frac{\pi}{4}}}{\sqrt{8k\pi}} \left(e^{-i\frac{\pi}{4}}\sqrt{\frac{k}{2\pi}}\right)^{n-2} \frac{e^{ikr}}{r^{\frac{n-1}{2}}} \left\{\sum_{m=1}^{M} \tau_j e^{-ik\hat{x}\cdot z_j} + \mathcal{O}\left(\frac{1}{r}\right)\right\} \quad \text{as } r := |x| \to \infty.$$

Therefore, the far field pattern is given by

$$u^\infty(\hat{x}, k) = \sum_{m=1}^{M} \tau_m e^{-ik\hat{x}\cdot z_m}, \tag{2.5}$$

where $\hat{x} \in \mathbb{S}^{n-1} := \{x \in \mathbb{R}^n : |x| = 1\}$ denotes the observation direction.

Point-like scatterers. The second case is the scattering of plane waves by M point-like scatterers located at $z_1, z_2, \ldots, z_M \in \mathbb{R}^n$ in the homogeneous space $\mathbb{R}^n, n = 2, 3$. The incident plane wave u^i is of the form

$$u^i(x, \theta, k) = e^{ikx\cdot\theta}, \quad x \in \mathbb{R}^n, \tag{2.6}$$

where $\theta \in \mathbb{S}^{n-1}$ denotes the direction of propagation.

By neglecting all the multiple scattering between the scatterers, the scattered field u^s is given by [5]

$$u^s(x, \theta, k) = \sum_{m=1}^{M} \tau_m u^i(z_m, \theta, k)\Phi_k(x, z_m), \tag{2.7}$$

which solves the equation $\Delta u^s(x,\theta,k) + k^2 u^s(x,\theta,k) = \sum_{m=1}^{M} \tau_m u^i(z_m,\theta,k)\delta_{z_m}$ in $\mathbb{R}^n$. Here, $\tau_m \in \mathbb{C}\backslash\{0\}$ is the scattering strength of the mth target, $m = 1, 2, \ldots, M$. Similarly, the far field pattern is given by

$$u^\infty(\hat{x}, \theta, k) = \sum_{m=1}^{M} \tau_m e^{-ik(\hat{x}-\theta)\cdot z_m}, \quad \hat{x}, \theta \in \mathbb{S}^{n-1}. \tag{2.8}$$

The backscattering case is of particularly interest, i.e., $\hat{x} = -\theta$.

In both cases, for a finite number $L \in \mathbb{N}$, we denote by

$$\Gamma := \{x_1, x_2, \ldots, x_L\} \subset \mathbb{R}^n\backslash\{z_1, z_2, \ldots, z_M\}$$

and

$$\Theta_L := \{\hat{x}_1, \hat{x}_2, \ldots, \hat{x}_L\} \in \mathbb{S}^{n-1}, \tag{2.9}$$

respectively, the collection of the sensors for the scattered fields and the far field patterns. The inverse problem we are interested in is to identify the locations and scattering strengths of the unknown point objects from the multifrequency scattered fields or far fields at a few sensors.

3. Uniqueness. In this section, we investigate under what conditions a target can be uniquely determined by a knowledge of its scattered fields or far field patterns. We note that by analyticity both the scattered field and its far field pattern are completely determined for all positive frequencies by only knowing them in some bounded band as given in (2.1).

We begin with the simplest case with a single point source, i.e., $M = 1$. In this case, the scattered field and its far field are given, respectively, by

$$u^s(x,k) = \tau_1 \Phi_k(x, z_1) \quad \text{and} \quad u^\infty(\hat{x}, k) = \tau_1 e^{-ik\hat{x}\cdot z_1}. \tag{3.1}$$

THEOREM 3.1. *For a fixed frequency $k > 0$, let $M = 1$; then we have the following results:*

- *For any fixed sensor $\hat{x} \in \mathbb{S}^{n-1}$, $n = 2, 3$, or $x \in \mathbb{R}^3 \backslash \{z_1\}$, we have*

$$\tau_1 = u^\infty(\hat{x}, k) e^{ik\hat{x}\cdot z_1}, \qquad |x - z_1| = \frac{|\tau_1|}{4\pi |u^s(x,k)|}. \tag{3.2}$$

- *If we know the location z_1 in advance, then the strength τ_1 is uniquely determined by the scattered field $u^s(x,k)$ at a single sensor $x \in \mathbb{R}^n \backslash \{z_1\}$ or by the far field pattern $u^\infty(\hat{x}, k)$ at a single observation direction $\hat{x} \in \mathbb{S}^{n-1}$, $n = 2, 3$.*
- *If we know the scattering strength τ_1 in advance, under the condition that $|k\hat{x}\cdot z_1| < \pi$, then the value $\hat{x}\cdot z_1$ is uniquely determined by the far field pattern $u^\infty(\hat{x}, k)$ at a single observation direction $\hat{x} \in \mathbb{S}^{n-1}$, $n = 2, 3$. Furthermore, the location $z_1 \in \mathbb{R}^n$ can be uniquely determined by n linearly independent observation directions.*
- *If we know the modulus $|\tau_1|$ in advance, then the distance $|x - z_1|$ is uniquely determined by the phaseless scattered field $|u^s(x,k)|$ at a fixed sensor $x \in \mathbb{R}^3$. Furthermore, the location $z_1 \in \mathbb{R}^3$ can be uniquely determined by four sensors $x_1, x_2, x_3, x_4 \in \mathbb{R}^3 \backslash \{z_1\}$, which are not coplanar.*

Proof. The first three results are obvious from the representation (3.1) of the scattered field and its far field pattern. If the modulus $|\tau_1|$ is given in advance, this implies that the location

$$z_1 \in \partial B_{r_j}(x_j),$$

where $\partial B_{r_j}(x_j)$ is a sphere centered at the sensor x_j with radius $r_j := \frac{|\tau_1|}{4\pi |u^s(x_j,k)|}$, $j = 1, 2, 3, 4$. We give a constructive proof for the determination of z_1. With the first two sensors x_1 and x_2, we obtain that z_1 is located on the circle $\partial B_{r_1}(x_1) \cap \partial B_{r_2}(x_2)$, which is the intersection of two spheres $\partial B_{r_1}(x_1)$ and $\partial B_{r_2}(x_2)$. Since the four sensors x_1, x_2, x_3, and x_4 are not coplanar, we have that x_1, x_2, and x_3 are not collinear. This implies that the circle $\partial B_{r_1}(x_1) \cap \partial B_{r_2}(x_2)$ and the sphere $\partial B_{r_3}(x_3)$ intersect at two points $\{A, B\}$. If $A = B$, then A is exactly the position z_1 we are looking for. Otherwise, $|x_4 - A| \neq |x_4 - B|$ because x_4 is not in the plane passing through x_1, x_2, and x_3. Thus $z_1 = A$ if $r_4 = |x_4 - A|$, or else $z_1 = B$. ∎

Note that the second equality in (3.2) does not hold in $\mathbb{R}^2$, and therefore the fourth result in Theorem 3.1 is not clear in two dimensions. Actually, we claim that the modulus $|H_0^{(1)}(t)|$ is monotonous with respect to the variable t. Numerical experiments indicate that this is indeed the case, but a rigorous proof is not known. If this is correct, we can show that the distance $|x-z|$ in $\mathbb{R}^2$ can be uniquely determined by the modulus $|u^s(x,k)|$, and therefore the location z can be uniquely determined by the phaseless data $|u^s(x,k)|$ at three sensors that are not collinear. This procedure is based on the phase retrieval technique proposed in the recent works [9, 10, 11].

The following theorem shows that both the location z_1 and the strength τ_1 can be uniquely determined by the multifrequency data.

THEOREM 3.2. *For all $k \in (k_-, k_+)$ and for $M = 1$, we have the following results:*

- *In $\mathbb{R}^3$, assume that $u^s(x,k_-) \neq u^s(x,k_+)$ at four sensors $x_1, x_2, x_3, x_4 \in \mathbb{R}^3\backslash\{z_1\}$, which are not coplanar. Then both z_1 and τ_1 can be uniquely determined by the multifrequency scattered fields $u^s(x,k)$, $x \in \{x_1, x_2, x_3, x_4\}$, $k \in (k_-, k_+)$.*
- *In $\mathbb{R}^n$, assume that $u^\infty(\hat{x},k_-) \neq u^\infty(\hat{x},k_+)$ at n linearly independent observation directions $\hat{x}_1, \hat{x}_2, \ldots, \hat{x}_n$, $n = 2, 3$. Then both z_1 and τ_1 can be uniquely determined by the multifrequency far field patterns $u^\infty(\hat{x},k)$, $k \in (k_-, k_+)$, at n linearly independent observation directions $\hat{x}_1, \hat{x}_2, \ldots, \hat{x}_n$, $n = 2, 3$.*

Proof. By the representation (3.1) for the scattered field, we have

$$\frac{u^s(x,k)}{u^s(x,k_-)} = e^{i(k-k_-)|x-z_1|}, \quad x \in \{x_1, x_2, x_3, x_4\},\ k \in (k_-, k_+).$$

Taking the integral on both sides with respect to k over the frequency band (k_-, k_+), we have

$$\begin{aligned}\int_{k_-}^{k_+} \frac{u^s(x,k)}{u^s(x,k_-)} dk &= \int_{k_-}^{k_+} e^{i(k-k_-)|x-z_1|} dk \\ &= \frac{1}{i|x-z_1|}\left[e^{i(k_+-k_-)|x-z_1|} - 1\right] \\ &= \frac{-i}{|x-z_1|}\left[\frac{u^s(x,k_+)}{u^s(x,k_-)} - 1\right], \quad x \in \{x_1, x_2, x_3, x_4\}.\end{aligned}$$

This implies that

$$|x-z_1| = -i\frac{\frac{u^s(x,k_+)}{u^s(x,k_-)} - 1}{\int_{k_-}^{k_+} \frac{u^s(x,k)}{u^s(x,k_-)} dk}, \quad x \in \{x_1, x_2, x_3, x_4\}. \tag{3.3}$$

Note that our assumption on the scattered fields ensures that both the numerator and the denominator of the right-hand side are nonzeros. Thus τ_1 can be uniquely recovered by (3.1). Since the distances $|x-z_1|$, $x \in \{x_1, x_2, x_3, x_4\}$, are uniquely determined, one can recover the location z_1 similarly as in Theorem 3.1.

Now we turn to the far field measurements. Similarly, by the representation (3.1) for the far field pattern, we have

$$\frac{u^\infty(\hat{x},k)}{u^\infty(\hat{x},k_1)} = e^{-i(k-k_1)\hat{x}\cdot z_1}, \quad \hat{x} \in \{\hat{x}_1, \ldots, \hat{x}_n\},\ k \in (k_-, k_+).$$

Multiplying this identity by $-i\hat{x}\cdot z_1$ and integrating over (k_-, k_+), we obtain

$$\begin{aligned}-i\hat{x}\cdot z_1\int_{k_-}^{k_+}\frac{u^\infty(\hat{x},k)}{u^\infty(\hat{x},k_-)}dk &= -i\hat{x}\cdot z_1\int_{k_-}^{k_+}e^{-i(k-k_-)\hat{x}\cdot z_1}dk\\ &= e^{-i(k_+-k_-)\hat{x}\cdot z_1}-1\\ &= \frac{u^\infty(\hat{x},k_+)}{u^\infty(\hat{x},k_-)}-1,\quad \hat{x}\in\{\hat{x}_1,\dots,\hat{x}_n\}.\end{aligned}$$

This implies that

$$\hat{x}\cdot z_1 = i\frac{\frac{u^\infty(\hat{x},k_+)}{u^\infty(\hat{x},k_-)}-1}{\int_{k_-}^{k_+}\frac{u^\infty(\hat{x},k)}{u^\infty(\hat{x},k_-)}dk},\quad \hat{x}\in\{\hat{x}_1,\dots,\hat{x}_n\}. \tag{3.4}$$

The scattering strength τ_1 is then uniquely determined by combining (3.1). The identity (3.4) also implies that z_1 is uniquely determined by noting the fact that the observation directions $\hat{x}_1, \hat{x}_2$, and $\hat{x}_n$ are linearly independent. ∎

Difficulties arise if there is more than one point source, i.e., $M > 1$. This is due to the severe nonlinearity between the measurements and the locations of the point sources. Note that

$$\Pi_{l,m}:\quad \hat{x}_l\cdot(z-z_m)=0 \tag{3.5}$$

is the hyperplane passing through the location z_m, $m = 1, 2, \dots, M$, with normal $\hat{x}_l \in \Theta_L$, $l = 1, 2, \dots, L$. For any point $z \in \mathbb{R}^n$, denote by $f(z)$ the number of the hyperplanes $\Pi_{l,m}$, $l = 1, 2, \dots, L$, $m = 1, 2, \dots, M$, passing through z.

LEMMA 3.3. *We consider M points $z_1, z_2, \dots, z_M$ in $\mathbb{R}^n$. Define*

$$L := \begin{cases} M+1 & \text{in } \mathbb{R}^2;\\ 2M+1 & \text{in } \mathbb{R}^3.\end{cases} \tag{3.6}$$

Recall the observation direction set $\Theta_L := \{\hat{x}_1, \hat{x}_2, \dots, \hat{x}_L\}$ and the hyperplanes $\Pi_{l,m}$ as in (3.5) for $l = 1, 2, \dots, L$ and $m = 1, 2, \dots, M$.

- *In $\mathbb{R}^2$, if any two directions in Θ_L are not collinear, then $f(z_m) = M + 1$, $m = 1, 2, \dots, M$, and $f(z) \le M$ for $z \in \mathbb{R}^2\backslash\{z_1, z_2, \dots, z_M\}$.*
- *In $\mathbb{R}^3$, if any three directions in Θ_L are not coplanar, then $f(z_m) = 2M + 1$, $m = 1, 2, \dots, M$, and $f(z) \le 2M$ for $z \in \mathbb{R}^3\backslash\{z_1, z_2, \dots, z_M\}$.*

Proof. In $\mathbb{R}^2$, since any two directions in Θ_L are not collinear, we obtain L hyperplanes $\Pi_{l,m}$, $l = 1, 2, \dots, L$, passing through z_m, $m = 1, 2, \dots, M$. Thus $f(z_m) = L = M + 1$, $m = 1, 2, \dots, M$. For any $z \in \mathbb{R}^2\backslash\{z_1, z_2, \dots, z_M\}$, the value $f(z)$ increases only if there is a hyperplane passing through z and some $z_m, m = 1, 2, \dots, M$, simultaneously. There are only M given points $z_m, m = 1, 2, \dots, M$. Therefore, for any $z \in \mathbb{R}^2\backslash\{z_1, z_2, \dots, z_M\}$, there are at most M hyperplanes passing through z. This implies that $f(z) \le M$ for $z \in \mathbb{R}^2\backslash\{z_1, z_2, \dots, z_M\}$.

In $\mathbb{R}^3$, since any three directions in Θ_L are not coplanar, we obtain L hyperplanes $\Pi_{l,m}$, $l = 1, 2, \dots, L$, passing through z_m, $m = 1, 2, \dots, M$. Thus $f(z_m) = L = 2M + 1$, $m = 1, 2, \dots, M$. It is clear that $f(z) \le L$ for all $z \in \mathbb{R}^3$. Assume that there exists a point $z^* \in \mathbb{R}^3\backslash\{z_1, z_2, \dots, z_M\}$ such that $f(z^*) = L$. Then for each observation direction $\hat{x}_l$, there exists some $z_m \in \{z_1, z_2, \dots, z_M\}$ such that $\hat{x}_l \cdot (z^* - z_m) = 0$, $l = 1, 2, \dots, 2M + 1$. By the pigeonhole principle, there exist one point

$z_m \in \{z_1, z_2, \ldots, z_M\}$ and three different observation directions $\hat{x}_{l_1}$, $\hat{x}_{l_2}$, and $\hat{x}_{l_3}$ such that $\hat{x} \cdot (z^* - z_m) = 0$ for $\hat{x} \in \{\hat{x}_{l_1}, \hat{x}_{l_2}, \hat{x}_{l_3}\}$. Therefore the observation directions $\hat{x}_{l_1}$, $\hat{x}_{l_2}$, and $\hat{x}_{l_3}$ are coplanar. This leads to a contradiction of our assumption on the observation directions, completing the proof. ∎

With the results given in Lemma 3.3, we can determine the locations and scattering strengths of the point sources by the multifrequency far field patterns at finitely many observation directions.

THEOREM 3.4. *We consider M isolated point sources with locations $z_m \in \mathbb{R}^n$ and scattering strengths $\tau_m \in \mathbb{C}\backslash\{0\}$, $m = 1, 2, \ldots, M$. Recall L defined by* (3.6) *and the observation direction set $\Theta_L := \{\hat{x}_1, \hat{x}_2, \ldots, \hat{x}_L\} \subset \mathbb{S}^{n-1}$. Consider the same assumptions on the observation directions as in Lemma* 3.3. *Then we have the following uniqueness results:*

- *The locations z_m and scattering strengths τ_m, $m = 1, 2, \ldots, M$, can be uniquely determined by the far field patterns $u^\infty(\pm\hat{x}, k)$ for all $\hat{x} \in \Theta_L$ and $k \in (k_-, k_+)$.*
- *If we further assume that $\tau_m \in \mathbb{R}$, then locations z_m and scattering strengths τ_m, $m = 1, 2, \ldots, M$, can be uniquely determined by the far field patterns $u^\infty(\hat{x}, k)$ for all $\hat{x} \in \Theta_L$ and $k \in (k_-, k_+)$.*

Proof. Note that the far field pattern $u^\infty(\hat{x}, k) = \sum_{m=1}^M \tau_m e^{-ik\hat{x}\cdot z_m}$ depends analytically on k, and thus we have the far field patterns for all frequencies in $(0, \infty)$. Integrating with respect to k, we deduce that

$$\begin{aligned}\int_0^\infty \Big(u^\infty(\hat{x}, k) + u^\infty(-\hat{x}, k)\Big)dk &= \int_0^\infty \sum_{m=1}^M \tau_m \Big(e^{-ik\hat{x}\cdot z_m} + e^{ik\hat{x}\cdot z_m}\Big)dk \\ &= \sum_{m=1}^M \tau_m \int_{-\infty}^\infty e^{-ik\hat{x}\cdot z_m} dk \\ &= 2\pi \sum_{m=1}^M \tau_m \delta(\hat{x} \cdot z_m), \quad \hat{x} \in \Theta_L,\end{aligned}$$

where δ is the Dirac delta function. This implies that for each $\hat{x} \in \Theta_L$, the values $\hat{x} \cdot z_m$, $m = 1, 2, \ldots, M$, are given uniquely by the far field patterns $u^\infty(\pm\hat{x}, k)$ for all $\hat{x} \in \Theta_L$ and $k > 0$. From this, we can then define the hyperplanes $\Pi_{l,m} : \hat{x}_l \cdot (z - z_m) = 0$, $l = 1, 2, \ldots, L$, $m = 1, 2, \ldots, M$. Using Lemma 3.3, we deduce that z_m, $m = 1, 2, \ldots, M$, can be uniquely recovered by the far field patterns $u^\infty(\pm\hat{x}, k)$ for all $\hat{x} \in \Theta_L$ and $k > 0$. For any $z_{m^*} \in \{z_1, z_2, \ldots, z_M\}$, by the assumption on the observation directions, we can always choose some $\hat{x}_l \in \Theta_L$ such that $\hat{x}_l \cdot (z_{m^*} - z_m) \neq 0$ for all $z_m \neq z_{m^*}$, $m = 1, 2, \ldots, M$. Then by the representation of the far field pattern, we have

$$u^\infty(\hat{x}_l, k) e^{ik\hat{x}_l \cdot z_{m^*}} = \tau_{m^*} + \sum_{m=1, m\neq m^*}^M \tau_m e^{-ik\hat{x}_l \cdot (z_m - z_{m^*})}.$$

For any $K > 0$,

$$\begin{aligned}&\int_0^K \Big(u^\infty(\hat{x}_l, k) e^{ik\hat{x}_l \cdot z_{m^*}} + u^\infty(-\hat{x}_l, k) e^{-ik\hat{x}_l \cdot z_{m^*}}\Big)dk \\ &= 2K\tau_{m^*} + \sum_{m=1, m\neq m^*}^M \tau_m \int_{-K}^K e^{-ik\hat{x}_l \cdot (z_m - z_{m^*})} dk.\end{aligned}$$

Letting $K \to \infty$, we obtain that the second term on the right-hand side of the above equality tends to $2\pi \sum_{m=1, m\neq m^*}^{M} \tau_m \delta(\hat{x}_l \cdot (z_m - z_{m^*}))$ and therefore vanishes since $\hat{x}_l \cdot (z_{m^*} - z_m) \neq 0$ for all $z_m \neq z_{m^*}$, $m = 1, 2, \ldots, M$. This implies

$$\tau_m = \lim_{K\to\infty} \frac{1}{2K} \int_0^K \left(u^\infty(\hat{x}_l, k) e^{ik\hat{x}_l \cdot z_m} + u^\infty(-\hat{x}_l, k) e^{-ik\hat{x}_l \cdot z_m} \right) dk.$$

In other words, τ_m, $m = 1, 2, \ldots, M$, are also uniquely determined by the far field patterns $u^\infty(\pm\hat{x}, k)$ for all $\hat{x} \in \Theta_L$ and $k > 0$. This completes the proof for the first statement.

If we further assume that $\tau_m \in \mathbb{R}$, then we need less data, as given in the second statement. In this case, we define

$$u^\infty(\hat{x}, k) := \overline{u^\infty(\hat{x}, -k)}, \quad k < 0,$$

where by $\bar{\cdot}$ we denote the complex conjugate. Then the proof follows by similar arguments. ∎

Inspired by the arguments in [6], uniqueness can also be established by finitely many properly chosen frequencies. For a fixed observation direction $\hat{x} \in \Theta_L$, assume that the far field patterns $u^\infty(\hat{x}, k_j)$ in (2.5) are given for J equidistant wave numbers

$$k_j = jk_{min}, \quad j = 1, 2, \ldots, J, \tag{3.7}$$

where

$$0 < k_{min} \leq \frac{\pi}{2R} \quad \text{and} \quad J > 2M. \tag{3.8}$$

Here, $R > 0$ denotes the radius of the smallest ball centered at the origin that contains the locations of the point sources. The upper bound on k_{min} in (3.8) implies that $|k_{min}\hat{x} \cdot z_m| < \pi$ for all $m = 1, 2, \ldots, M$. This further implies that the value $\hat{x} \cdot z_m$ is uniquely determined by $e^{-ik_{min}\hat{x}\cdot z_m}$. In the following we develop a rigorous characterization of the projections $\hat{x} \cdot z_m$, $m = 1, 2, \ldots, M$, from the far field patterns $u^\infty(\hat{x}, k_j), j = 1, 2, \ldots, J$.

For a fixed observation direction $\hat{x}$ different locations $z_{m_1} \neq z_{m_2}$ may yield the same projections $\hat{x} \cdot z_{m_1} = \hat{x} \cdot z_{m_2}$, and the corresponding summands in (2.5) even cancel out if $\tau_{m_1} = -\tau_{m_2}$. In this case, the point sources at z_{m_1} and z_{m_2} would not contribute to the far field data $u^\infty(\hat{x}, k_j), j = 1, 2, \ldots, J$, and consequently they can not be reconstructed from such far field data. We introduce the set and its cardinality

$$\mathcal{M}_{\hat{x}} := \operatorname{supp}\left(\sum_{m=1}^{M} \tau_m \delta(\hat{x} \cdot z_m) \right) \subset \mathbb{R}, \quad M^* := |\mathcal{M}_{\hat{x}}|.$$

Clearly, $M^* \leq M$. Accordingly, we rewrite the far field patterns as

$$u^\infty(\hat{x}, k_j) = \sum_{m=1}^{M^*} \tau_m^* \xi_m^j, \quad j = 1, 2, \ldots, J, \tag{3.9}$$

where $\xi_m := e^{-ik_{min}f_m}$ for any $f_m \in \mathcal{M}_{\hat{x}}$. The far field patterns $u^\infty(\hat{x}, k_j), j = 1, 2, \ldots, J$, define the Hankel matrix

$$U := \begin{pmatrix} u^\infty(\hat{x}, k_1) & u^\infty(\hat{x}, k_2) & \cdots & u^\infty(\hat{x}, k_{M+1}) \\ u^\infty(\hat{x}, k_2) & u^\infty(\hat{x}, k_3) & \cdots & u^\infty(\hat{x}, k_{M+2}) \\ \vdots & \vdots & \ddots & \vdots \\ u^\infty(\hat{x}, k_{J-M}) & u^\infty(\hat{x}, k_{J-M+1}) & \cdots & u^\infty(\hat{x}, k_J) \end{pmatrix} \in \mathbb{C}^{(J-M)\times(M+1)}.$$

LEMMA 3.5. *The Hankel matrix U has a factorization of the form*

$$U = V_{J-M} D V_{M+1}^{\top}, \tag{3.10}$$

where $V_{\mathbb{i}} = (v_1, v_2, \ldots, v_{M^*}) \in \mathbb{C}^{\mathbb{i} \times M^*}, \mathbb{i} \geq 2$, denotes a Vandermonde matrix with $v_m = (1, \xi_m, \xi_m^2, \ldots, \xi_m^{\mathbb{i}-1})^{\top}$ for $m = 1, 2, \ldots, M^*$, and the matrix $D = \operatorname{diag}(\tau_m^* \xi_m) \in \mathbb{C}^{M^* \times M^*}$. Furthermore,

$$\operatorname{rank}(U) = \operatorname{rank}(V_{J-M}) = \operatorname{rank}(V_{M+1}) = M^* \tag{3.11}$$

and

$$\mathcal{R}(U) = \mathcal{R}(V_{J-M}). \tag{3.12}$$

Proof. The factorization (3.10) follows by a straightforward calculation. Since $\xi_1, \xi_2, \ldots, \xi_{M^*}$ are mutually distinct by construction, the rank of the Vandermonde matrix $V_{\mathbb{i}} \in \mathbb{C}^{\mathbb{i} \times M^*}$ satisfies

$$\operatorname{rank}(V_{\mathbb{i}}) = \min\{\mathbb{i}, M^*\}.$$

Therefore, we deduce from the assumption $J > 2M \geq 2M^*$ that

$$\operatorname{rank}(V_{J-M}) = \operatorname{rank}(V_{M+1}) = M^*.$$

Clearly, $D \in \mathbb{C}^{M^* \times M^*}$ is invertible, and thus the factorization (3.10) implies

$$\operatorname{rank}(U) = M^*.$$

Finally, we show the range identity (3.12). It is clear that $\mathcal{R}(U) \subset \mathcal{R}(V_{J-M})$ from the factorization (3.10). Conversely, assume that

$$\phi = V_{J-M} \psi$$

for some $\psi \in \mathbb{C}^{M^* \times 1}$. Using the invertibility of D again, we denote by

$$\psi^* := D^{-1} \psi.$$

Note that $\operatorname{rank}(V_{M+1}) = M^*$; we can always find some $\eta \in \mathbb{C}^{(M+1) \times 1}$ such that

$$\psi^* = V_{M+1}^{\top} \eta.$$

Combining the previous identities, we deduce that $U\eta = V_{J-M} D V_{M+1}^{\top} \eta = V_{J-M} D \psi^* = V_{J-M} \psi = \phi$, i.e., $\phi \in \mathcal{R}(U)$. This finishes the proof. ∎

THEOREM 3.6. *For a single observation direction $\hat{x} \in \mathbb{S}^{n-1}$, the hyperplanes $\Pi_m : \hat{x} \cdot (z - z_m) = 0$, $m = 1, 2, \ldots, M$, are uniquely determined by the far field patterns $u^{\infty}(\hat{x}, k_j)$, $j = 1, 2, \ldots, J$.*

Proof. Let B_R be the ball centered at the origin with radius R. For a point $z \in B_R \subset \mathbb{R}^n$, define $\xi := e^{-ik_{min}\hat{x} \cdot z}$ and $\phi_z := (1, \xi, \xi^2, \ldots, \xi^{J-M-1})^{\top} \in \mathbb{C}^{(J-M) \times 1}$. We claim that $\phi_z \in \mathcal{R}(U)$ if and only if $\xi \in \{\xi_1, \xi_2, \ldots, \xi_{M^*}\}$.

First, let $\xi \in \{\xi_1, \xi_2, \ldots, \xi_{M^*}\}$. Then clearly $\phi_z \in \mathcal{R}(V_{J-M})$ by the construction of the matrix V_{J-M}. The range identity (3.12) in Lemma 3.5 implies that $\phi_z \in \mathcal{R}(U)$.

Now let $\xi \notin \{\xi_1, \xi_2, \ldots, \xi_{M^*}\}$. The assumption $J > 2M$ implies that $J - M > M + 1 > M^* + 1$. Then the novel Vandermonde matrix $(V_{J-M}, \phi_z) \in \mathbb{C}^{(J-M) \times (M^*+1)}$ has rank $M^* + 1$. This implies that $\phi_z \notin \mathcal{R}(V_{J-M})$ and consequently $\phi_z \notin \mathcal{R}(U)$ by using (3.12) again.

If $\phi_z \in \mathcal{R}(U)$, then $\xi = \xi_m$ for some $1 \leq m \leq M$, i.e., $e^{-ik_{min}\hat{x} \cdot z} = e^{-ik_{min}\hat{x} \cdot z_m}$. By the assumption (3.8) of the smallest wave number k_{min}, we deduce that $\hat{x} \cdot z = \hat{x} \cdot z_m$. That is, the hyperplane $\Pi_m : \ \hat{x} \cdot (z - z_m) = 0$ is uniquely determined. ∎

Combining Theorem 3.6 and Lemma 3.3, we immediately have the following uniqueness results on the determination of the locations by the far field patterns with finitely many observation directions and finitely many frequencies.

THEOREM 3.7. *Let k_j be the wave number given by* (3.7) *satisfying* (3.8). *Letting L be given as in* (3.6), *we consider L observation directions $\hat{x}_l, l = 1, 2, \ldots, L$, satisfying the same conditions as in Lemma* 3.3. *Then the locations $z_1, z_2, \ldots, z_M$ can be uniquely determined by the far field patterns $u^\infty(\hat{x}_l, k_j)$, $l = 1, 2, \ldots, L$, $j = 1, 2, \ldots, J$.*

Having reconstructed the locations of the point sources, we show in the following theorem that the corresponding scattering strengths can be uniquely determined by the multifrequency far field patterns at some fixed observation direction.

THEOREM 3.8. *Let k_j be the wave number given by* (3.7) *satisfying* (3.8). *Let $\hat{x} \in \mathbb{S}^{n-1}$ be such that $\hat{x} \cdot (z_{m_1} - z_{m_2}) \neq 0$ if $m_1 \neq m_2$. Given the locations $z_1, z_2, \ldots, z_M$, the corresponding scattering strengths $\tau_1, \tau_2, \ldots, \tau_M$ can be uniquely determined by the multifrequency far field patterns $u^\infty(\hat{x}, k_j)$, $j = 1, 2, \ldots, J$, at the fixed observation direction $\hat{x}$.*

Proof. Recall that the far field patterns are given by

$$u^\infty(\hat{x}, k_j) = \sum_{m=1}^{M} \tau_m \eta_m^j, \quad j = 1, 2, \ldots, J, \tag{3.13}$$

where $\eta_m := e^{-ik_{min}\hat{x}\cdot z_m}$. We rewrite equations (3.13) in the matrix form

$$\mathbb{V}\mathbb{T} = \mathbb{U}, \tag{3.14}$$

where $\mathbb{T} = (\tau_1, \tau_2, \ldots, \tau_M)^\top$, $\mathbb{V} = (\mathbb{v}_1, \mathbb{v}_2, \ldots, \mathbb{v}_M) \in \mathbb{C}^{J\times M}$ denotes a Vandermonde matrix with $\mathbb{v}_m = (\eta_m, \eta_m^2, \ldots, \eta_m^J)^\top$, $m = 1, 2, \ldots, M$, and $\mathbb{U} = (u^\infty(\hat{x}, k_1), u^\infty(\hat{x}, k_2), \ldots, u^\infty(\hat{x}, k_J))^\top$. Since $\eta_1, \eta_2, \ldots, \eta_M$ are distinct by the assumption on $\hat{x}$, we have that

$$\operatorname{rank}(\mathbb{V}) = \min\{J, M\} = M.$$

Therefore, (3.14) is uniquely solvable. In other words, the scattering strengths $\tau_1, \tau_2, \ldots, \tau_M$ can be uniquely determined by the far field patterns $u^\infty(\hat{x}, k_j)$, $j = 1, 2, \ldots, J$. The proof is complete. ∎

Finally, we turn to the scattering of plane waves by point-like scatterers. Recall that the scattered field and the corresponding far field pattern are given by

$$u^s(x, \theta, k) = \sum_{m=1}^{M} \tau_m u^i(z_m, \theta, k)\Phi_k(x, z_m), \quad x \in \mathbb{R}^n \backslash \{z_1, z_2, \ldots, z_M\},$$

and

$$u^\infty(\hat{x}, \theta, k) = \sum_{m=1}^{M} \tau_m e^{-ikz_m\cdot(\hat{x}-\theta)}, \quad \hat{x}, \theta \in \mathbb{S}^{n-1},$$

respectively. We collect the uniqueness results in the following theorem. We omit the proof since it is similar to the case of inverse source scattering problems.

THEOREM 3.9. *We consider the scattering of plane waves by point-like scatterers. Then we have the following uniqueness results.*

$M = 1$

- *Let $k > 0$ be fixed. For any single sensor $\hat{x} \in \mathbb{S}^{n-1}$ or $x \in \mathbb{R}^3 \backslash \{z_1\}$, we have*

$$\tau_1 = u^\infty(\hat{x}, \theta, k) e^{ikz_1 \cdot (\hat{x} - \theta)}, \qquad |x - z_1| = \frac{|\tau_1|}{4\pi |u^s(x, \theta, k)|}. \tag{3.15}$$

- *Let $k > 0$ be fixed. If we know the location z_1 in advance, then the strength τ_1 is uniquely determined by the scattered field $u^s(x, \theta, k)$ at a single sensor $x \in \mathbb{R}^n \backslash \{z_1\}$ or the far field pattern $u^\infty(\hat{x}, \theta, k)$ at a single observation direction $\hat{x} \in \mathbb{S}^{n-1}$.*
- *Let $k > 0$ be fixed. If we know the modulus $|\tau_1|$ in advance, then the location $z_1 \in \mathbb{R}^3$ is uniquely determined by the phaseless scattered field $|u^s(x, \theta, k)|$ at four sensors $x_1, x_2, x_3, x_4 \in \mathbb{R}^3 \backslash \{z_1\}$, which are not coplanar.*
- *In $\mathbb{R}^3$, both the location z_1 and the strength τ_1 can be uniquely determined by the multifrequency scattered fields $u^s(x, \theta, k), k \in (k_-, k_+)$, at four sensors $x_1, x_2, x_3, x_4 \in \mathbb{R}^3 \backslash \{z_1\}$, which are not coplanar.*
- *In $\mathbb{R}^n$, both the location z_1 and the strength τ_1 can be uniquely determined by the multifrequency far field patterns $u^\infty(\hat{x}, \theta, k), k \in (k_-, k_+)$, at n pairs of linearly independent directions $\phi_j := \hat{x}_j - \theta_j$, $j = 1, 2, \ldots, n$.*

$M > 1$ *Recall L and Θ_L defined by (3.6) and (2.9), respectively. Then we have the following results:*

- *The locations z_m and the scattering strengths τ_m, $m = 1, 2, \ldots, M$, can be uniquely determined by the far field patterns $u^\infty(\hat{x}, -\hat{x}, k)$ and $u^\infty(-\hat{x}, \hat{x}, k)$ for all $\hat{x} \in \Theta_L$ and $k \in (k_-, k_+)$.*
- *If we further assume that $\tau_m \in \mathbb{R}$, then locations z_m and scattering strengths τ_m, $m = 1, 2, \ldots, M$, can be uniquely determined by the far field patterns $u^\infty(\hat{x}, -\hat{x}, k)$ for all $\hat{x} \in \Theta_L$ and $k \in (k_-, k_+)$.*
- *We consider the following wave numbers:*

$$k_j = j k_{min}, \quad j = 1, 2, \ldots, J, \tag{3.16}$$

where

$$0 < k_{min} \leq \frac{\pi}{4R} \quad \text{and} \quad J > 2M. \tag{3.17}$$

Here, $R > 0$ denotes the radius of the smallest ball centered at the origin that contains the locations of the point-like scatterers. Then the locations z_m, $m = 1, 2, \ldots, M$, can be uniquely determined by the backscattering far field patterns $u^\infty(\hat{x}, -\hat{x}, k_j), j = 1, 2, \ldots, J$, at finitely many observation directions $\hat{x} \in \Theta_L$. Furthermore, taking $\hat{x} \in \mathbb{S}^{n-1}$ such that $\hat{x} \cdot z_{m_1} \neq \hat{x} \cdot z_{m_2}$ if $m_1 \neq m_2$, then the scattering strengths $\tau_m, m = 1, 2, \ldots, M$, can be uniquely determined by the far field patterns $u^\infty(\hat{x}, -\hat{x}, k_j), j = 1, 2, \ldots, J$, at the fixed observation direction $\hat{x}$.

4. Numerical methods. This section aims to introduce some novel numerical methods for identifying the locations and scattering strengths of the point object. Some of the numerical methods are originated from the constructive uniqueness proof in the previous section.

4.1. Numerical methods for point sources. We begin with the scattering by point sources. If $M = 1$, given $|\tau_1|$, we introduce the following indicator to locate

the position of z_1:

$$I_1(z) := \frac{1}{\sum_{j=1}^{4} \left| \frac{|x_j - z|}{|\tau_1|} - \frac{1}{4\pi |u^s(x_j, k)|} \right|}, \tag{4.1}$$

where x_j, $j = 1, 2, 3, 4$, are four points in $\mathbb{R}^3$ such that they are not coplanar. By the representation of the scattered field given in (2.3), we know that $I_1(z) \to \infty$ if $z \to z_1$. Thus $I_1(z)$ blows up at $z = z_1$.

The proof of Theorem 3.1 gives a constructive way to look for the position of z_1. Based on this, we introduce a simple geometrical method to reconstruct a point in $\mathbb{R}^3$ from four distances to the given points. The procedure is actually an extension of the geometrical method to reconstruct a point from three distances to the given points in $\mathbb{R}^2$, which is the key idea of phase retrieval [9, 10, 11]. However, the procedure for reconstructing a point in $\mathbb{R}^3$ is much more technical.

Let $x_j, j = 1, 2, 3, 4$, be four given points in $\mathbb{R}^3$ such that they are not coplanar, and denote $r_j := |x_j - z|$. The following scheme provides a constructive way for determining the unknown point z.

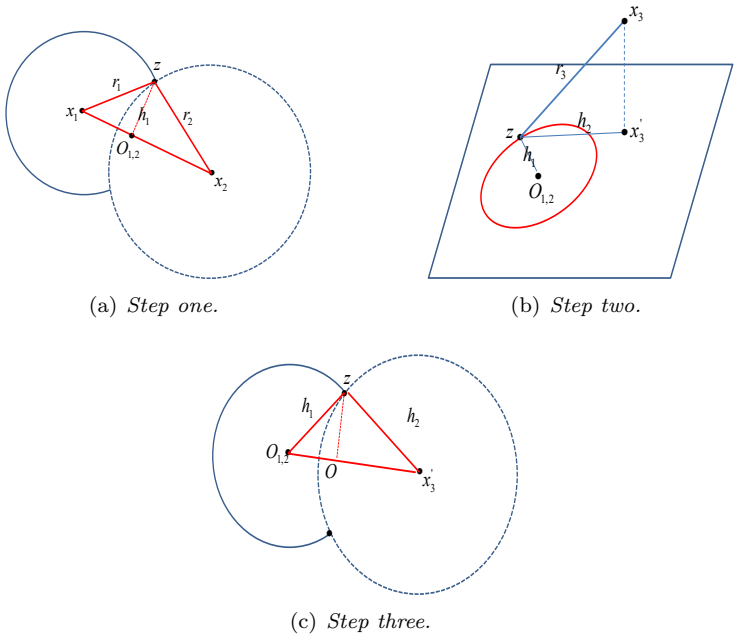

(a) *Step one.* (b) *Step two.*

(c) *Step three.*

FIG. 1. *Scheme for determining a point in* $\mathbb{R}^3$.

One-point determination scheme: Locating a point in $\mathbb{R}^3$ by four distances to the given points.

(1) Determine the perpendicular foot $O_{1,2}$ from two given points x_j, $j = 1, 2$, and two distances r_j, $j = 1, 2$.
As shown in Figure 1(a)*, by Heron's formula, the area of the triangle* $\Delta z x_1 x_2$ *is*

$$S_{\Delta z x_1 x_2} = \sqrt{p(p - r_1)(p - r_2)(p - |x_1 - x_2|)},$$

with $p := \frac{r_1+r_2+|x_1-x_2|}{2}$. *Noting* $S_{\Delta z x_1 x_2} = \frac{1}{2}|x_1 - x_2||z - O_{1,2}|$, *we deduce that*

$$h_1 := |z - O_{1,2}| = \frac{2S_{\Delta z x_1 x_2}}{|x_1 - x_2|}.$$

Then by the Pythagorean theorem, we have

$$|x_1 - O_{1,2}| = \sqrt{r_1^2 - h_1^2} = \sqrt{r_1^2 - \frac{4S^2_{\Delta z x_1 x_2}}{|x_1 - x_2|^2}}.$$

Denoting $t_1 := \frac{|x_1-O_{1,2}|}{|x_1-x_2|}$, *we have*

$$O_{1,2} = \begin{cases} x_1 + t_1(x_2 - x_1) & \text{if } r_1^2 + |x_1 - x_2|^2 \geq r_2^2; \\ x_1 - t_1(x_2 - x_1) & \text{else.} \end{cases}$$

(2) Determination of h_2 and the projection x_3'.

As shown in Figure 1(b), *noting that* x_3x_3' *is parallel to* x_1x_2, *we have*

$$x_3' = x_3 + t(x_1 - x_2),$$

with t *chosen such that* $(x_3'-O_{1,2})\cdot(x_1-x_2) = 0$. *By the Pythagorean theorem again, we have*

$$h_2 := |z - x_3'| = \sqrt{r_3^2 - |x_3 - x_3'|^2}.$$

(3) Determination of O.

As shown in Figure 1(c), *follow step one to reconstruct point* O.

(4) Determine the point z.

Define

$$l := \frac{(x_1 - x_2) \times (x_3' - O_{1,2})}{|(x_1 - x_2) \times (x_3' - O_{1,2})|}.$$

Then

$$z = O \pm t_2 l, \tag{4.2}$$

with $t_2 := \sqrt{h_1^2 - |O - O_{1,2}|^2}$. *We take* z *from* (4.2) *by letting* $|z - x_4| = r_4$.

Actually, even without knowing $|\tau_1|$, we can determine the distance between the sensor x and the unknown location z_1 by formula (3.3), i.e.,

$$|x - z_1| = -i\frac{\frac{u^s(x,k_+)}{u^s(x,k_-)} - 1}{\int_{k_-}^{k_+} \frac{u^s(x,k)}{u^s(x,k_-)} dk}, \quad x \in \{x_1, x_2, x_3, x_4\}. \tag{4.3}$$

The price to pay is more data with respect to the frequency k. Then one may locate z_1 by the above scheme. After determining the location z_1, the scattering strength τ_1 can be computed directly by the representation (2.3) of the scattered field $u^s(x, k)$ at any sensor x.

If the far field pattern is considered, we may determine $\hat{x} \cdot z_1$ by formula (3.4), i.e.,

$$\hat{x} \cdot z_1 = i\frac{\frac{u^\infty(\hat{x},k_+)}{u^\infty(\hat{x},k_-)} - 1}{\int_{k_-}^{k_+} \frac{u^\infty(\hat{x},k)}{u^\infty(\hat{x},k_-)} dk}, \quad \hat{x} \in \{\hat{x}_1, \ldots, \hat{x}_n\}. \tag{4.4}$$

Then z_1 can be determined by solving a system of linear equations with n unknowns in $\mathbb{R}^n$, $n = 2, 3$. In particular, one may take $\hat{x}$ to be the unit vectors in Cartesian coordinates. After this, the scattering strength can be computed by the representation (2.5) of the far field pattern.

We are more interested in the case with multiple point sources, i.e., $M > 1$. Define

$$I_M(z,\hat{x}) := \left| \int_0^K \left\{ u^\infty(\hat{x},k) e^{ik\hat{x}\cdot z} + u^\infty(-\hat{x},k) e^{-ik\hat{x}\cdot z} \right\} dk \right|, \quad z \in \mathbb{R}^n, \hat{x} \in \Theta_L. \tag{4.5}$$

By the analysis in the proof of Theorem 3.4, for large K, the indicator $I(z,\hat{x})$ blows up when the sampling point z is located on the hyperplanes $\hat{x}\cdot(z - z_m) = 0$, $m = 1, 2, \ldots, M$. Then we expect that the superposition of $I_M(z,\hat{x})$ with respect to $\hat{x} \in \Theta_L$ can be used to locate $z_m, m = 1, 2, \ldots, M$. Based on this idea, we define

$$I_M(z) := \sum_{\hat{x}\in\Theta_L} I_M(z,\hat{x}). \tag{4.6}$$

Numerically, $I_M(z)$ is expected to be large if $z = z_m$, $m = 1, 2, \ldots, M$, and small otherwise. After locating z_m, $m = 1, 2, \ldots, M$, we may compute the scattering strength with the help of the following formula:

$$\tau_m = \frac{1}{2K} \int_0^K \left\{ u^\infty(\hat{x},k) e^{ik\hat{x}\cdot z_m} + u^\infty(-\hat{x},k) e^{-ik\hat{x}\cdot z_m} \right\} dk, \quad m = 1, 2, \ldots, M. \tag{4.7}$$

Here, $\hat{x}$ is chosen such that $\hat{x}\cdot z_{m_1} \neq \hat{x}\cdot z_{m_2}$ if $m_1 \neq m_2$. As mentioned in the proof of Theorem 3.4, the right-hand side extends to τ_m as $K \to \infty$. Thus by taking K large enough, we hope to determine the scattering strength τ_m, $m = 1, 2, \ldots, M$.

To identify the points, we first locate the positions by I_M in (4.6) and then recover the scattering strengths by (4.7). In the subsequent numerical examples, as in the other sampling methods, we will choose a fine grid containing the unknown point objects.

4.2. Numerical methods for point-like scatterers. Now we turn to the scattering of plane waves by point-like scatterers. The indicator (4.1) with $u^s(x,k)$ replaced by $u^s(x,\theta,k)$ also works for locating a single point-like scatterer. As mentioned in the previous subsection, we are more interested in the case with multiple point-like scatterers. We need some modifications due to the incident plane waves. Of practical interest are the backscattering inverse scattering problems, i.e., $\hat{x} = -\theta$. By the backscattering far field patterns $u^\infty(\hat{x},-\hat{x},k)$ for $\hat{x} \in \Theta_L$ and $k \in (0,K)$, we define

$$\widetilde{I}_M(z,\hat{x}) := \left| \int_0^K \left\{ u^\infty(\hat{x},-\hat{x},k) e^{2ik\hat{x}\cdot z} + u^\infty(-\hat{x},\hat{x},k) e^{-2ik\hat{x}\cdot z} \right\} dk \right|, \quad z \in \mathbb{R}^n, \hat{x} \in \Theta_L. \tag{4.8}$$

Similarly, for large K, the indicator $\widetilde{I}_M(z,\hat{x})$ blows up when the sampling point z is located on the hyperplanes $\hat{x}\cdot(z - z_m) = 0$, $m = 1, 2, \ldots, M$. Then we further define

$$\widetilde{I}_M(z) := \sum_{\hat{x}\in\Theta_L} \widetilde{I}_M(z,\hat{x}). \tag{4.9}$$

TABLE 1
One-point source reconstruction using the scattered fields.

True point	$z_1 = (1,1,1)$ $\tau_1 = 1+i$	$z_2 = (1,0,1)$ $\tau_2 = 1-i$	$z_3 = (0,1,1)$ $\tau_3 = -1-i$
0 noise	$(1,1,1)$ $1.0024 + 0.9909i$	$(1,0,1)$ $0.9931 - 1.0012i$	$(0,1,1)$ $-0.9972 - 0.9947i$
2% noise	$(1,1,1)$ $0.9750 + 1.0094i$	$(0.95,-0.05,0.95)$ $0.9735 - 1.0055i$	$(0.05,1.05,1.05)$ $-1.0280 - 0.9947i$
5% noise	$(1,1,1)$ $1.0252 + 0.8692i$	$(0.9,-0.15,0.9)$ $0.9154 - 1.0180i$	$(-0.1,0.95,0.9)$ $-1.0787 - 0.8666i$
10% noise	$(1,1.05,1)$ $0.9313 + 1.1136i$	$(0.95,0.15,1)$ $0.8008 - 0.9240i$	$(-0.1,0.85,0.8)$ $-0.8865 - 1.2529i$

TABLE 2
Locating the point source by the one-point determination scheme.

True point	$z_1 = (1,1,1)$	$z_2 = (1,0,1)$	$z_3 = (0,1,1)$
0 noise	$(1,1,1)$	$(1,0,1)$	$(0,1,1)$
2% noise	$(0.99,1.02,0.99)$	$(1.04,0.01,1.05)$	$(-0.01,1.00,1.01)$
5% noise	$(0.92,0.88,0.90)$	$(1.11,0.14,1.03)$	$(0.04,1.00,0.96)$
10% noise	$(0.87,1.03,1.12)$	$(1.25,-0.11,1.09)$	$(-0.03,1.21,1.20)$

Again, $\widetilde{I}_M(z)$ is expected to be large if $z = z_m$, $m = 1, 2, \ldots, M$, and small otherwise. After locating z_m, $m = 1, 2, \ldots, M$, we compute the scattering strength using the following formula:

(4.10)
$$\tau_m = \frac{1}{2K} \int_0^K \left\{ u^\infty(\hat{x}, -\hat{x}, k) e^{2ik\hat{x}\cdot z_m} + u^\infty(-\hat{x}, \hat{x}, k) e^{-2ik\hat{x}\cdot z_m} \right\} dk, \quad m = 1, 2, \ldots, M.$$

5. Numerical examples and discussions. This section is devoted to some numerical examples to verify the effectiveness and robustness of the numerical methods proposed in the previous section. Note that both the theoretical results and numerical methods for the point obstacle case are quite similar to the point source case, and therefore we only present examples with point sources.

5.1. One point source. First, we consider the identification of one point source by the scattered fields at four sensors:

$$x_1 = (2,0,0), \quad x_2 = (0,2,0), \quad x_3 = (0,0,2), \quad \text{and} \quad x_4 = (-2,-2,-2).$$

The following three pairs of point sources with different locations and scattering strengths are considered:

- $z_1 = (1,1,1), \quad \tau_1 = 1+i;$
- $z_2 = (1,0,1), \quad \tau_2 = 1-i;$
- $z_3 = (0,1,1), \quad \tau_3 = -1-i.$

We first use (4.3) and (2.3) to get the strength, and then use the indicator (4.1) to capture the location of the point source. Table 1 gives the numerical results with different relative noise. In the numerical implementation, a trapezoid integral formula is applied with $k_- = 1, k_+ = 100, dk = 0.005$. Sampling space 0.05 is used in (4.1).

We also test a *one-point determination scheme* for the same points. Table 2 gives the results with varying noise.

Next, we consider the constructions using the far field patterns at three observa-

TABLE 3
One-point source reconstruction using the far fields.

True point	$z_1 = (1,1,1)$ $\tau_1 = 1+i$	$z_2 = (1,0,1)$ $\tau_2 = 1-i$	$z_3 = (0,1,1)$ $\tau_3 = -1-i$
0 noise	$(1,1,1)$ $0.9974 + 1.0026i$	$(1,0,1)$ $1.0026 - 0.9974i$	$(0,1,1)$ $-1.0000 - 1.0000i$
2% noise	$(0.99, 1.00, 1.00)$ $1.0279 + 1.0006i$	$(1.01, 0, 0.99)$ $1.0251 - 0.9981i$	$(0,1,1)$ $-1.0032 - 1.0032i$
5% noise	$(1.02, 0.99, 0.98)$ $1.0093 + 1.0480i$	$(0.98, 0, 1.00)$ $0.9753 - 1.0121i$	$(0, 1.00, 0.96)$ $-0.9793 - 0.9793i$
10% noise	$(1.08, 0.95, 0.94)$ $0.8724 + 1.0142i$	$(0.97, 0, 1.02)$ $1.0434 - 1.1004i$	$(0, 0.98, 1.04)$ $-0.9350 - 0.9350i$

tion directions,

$$\hat{x}_1 = (1,0,0), \quad \hat{x}_2 = (0,1,0), \quad \hat{x}_3 = (0,0,1).$$

Equations (4.4) and (2.5) are used to get the location and scattering strength, respectively. The results are summarized in Table 3 with varying noise.

5.2. Multiple point sources. In this part, more interesting cases with multiple point sources are considered. For simplicity, we present the examples in the two-dimensional case. The three-dimensional case is similar when using the same indicator. We first use (4.5) and (4.6) to locate the positions of the point sources; then (4.7) is used to get the strength. In what follows, if not stated otherwise, we take $k_- = 40$, $k_+ = 200$, $dk = 1$, and 10% relative noise in the numerical results. Sampling space 0.05 is used.

In the first example, we consider five point sources, located at

$$z_1 = (1,0), \quad z_2 = (0,1), \quad z_3 = (-1,0), \quad z_4 = (0,-1), \quad z_5 = (0,0).$$

We use the *rand* in MATLAB to set the true strengths. Figure 2 shows the reconstructions with one pair of directions. Clearly, the parallel lines containing the unknown points with normal in the observation direction are clearly reconstructed. To locate the points, we take 8 observation directions, $\hat{x}_j = (\cos\alpha_j, \sin\alpha_j)$, where $\alpha_j = 2\pi j/8, j = 0, \ldots, 7$. Figures 3(a) and 3(b) give the reconstruction of the five points using different frequency bands. The resolution is improved with more wave numbers. Table 4 gives the comparison of the true strength and the computed strength. For comparison, we also consider the following two point sets such that the points are closer to each other:

$$\mathscr{A} := \{(0.2,0),\ (0,0.2),\ (-0.2,0),\ (0,-0.2),\ (0,0)\},$$
$$\mathscr{B} := \{(0.1,0),\ (0,0.1),\ (-0.1,0),\ (0,-0.1),\ (0,0)\}.$$

As shown in Figures 3(c) and 3(d), the points are still well located. However, some flaws appear if the points are too close, as seen in point set $\mathscr{B}$.

In the second example, we use 35 points to characterize the word "AMSS" (abbreviation for Academy of Mathematics and Systems Science). All the strengths are set to 1. As shown in Figure 4, the 35 points are well captured, and even 10% relative noise is considered. In particular, for this complicated example, 32 equally distributed observation directions are used, where the direction number is smaller than the point number.

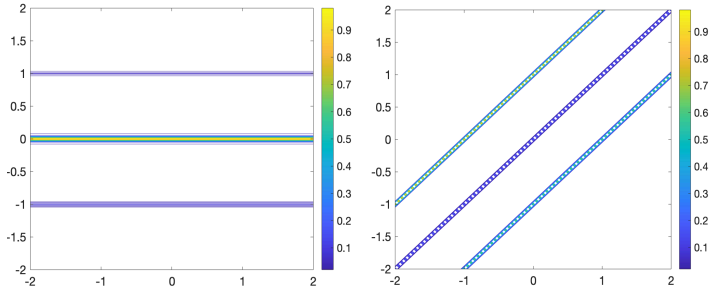

(a) $\hat{x} = \pm(0, 1)$.

(b) $\hat{x} = \pm(\frac{\sqrt{2}}{2}, -\frac{\sqrt{2}}{2})$.

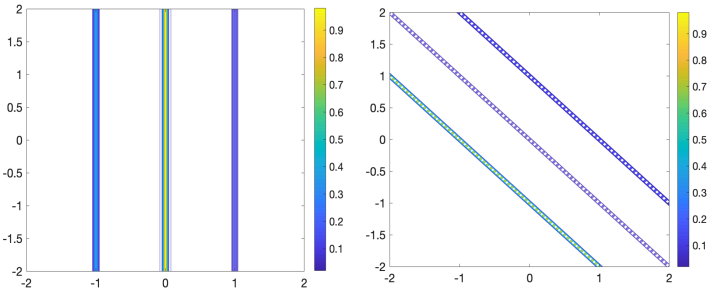

(c) $\hat{x} = \pm(1, 0)$.

(d) $\hat{x} = \pm(\frac{\sqrt{2}}{2}, \frac{\sqrt{2}}{2})$.

FIG. 2. *Reconstruction by* 2 *directions with* 10% *noise.*

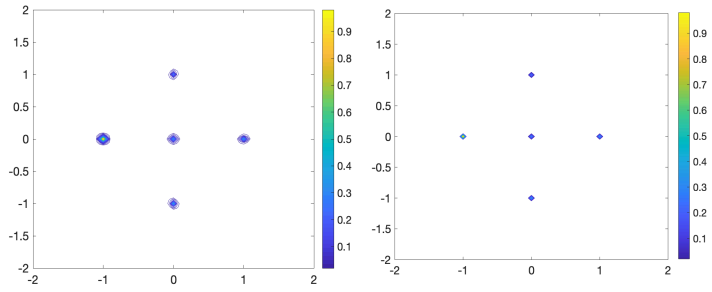

(a) $k \in (40, 100), dk = 1$.

(b) $k \in (40, 200), dk = 1$.

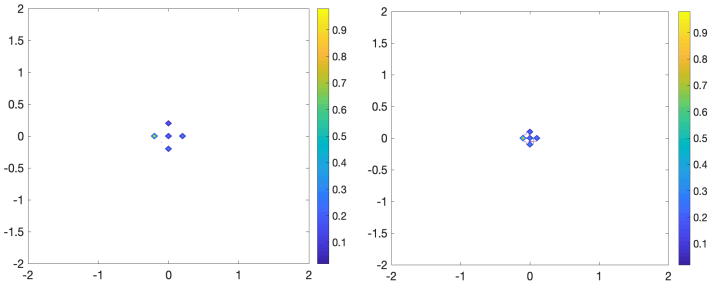

(c) *Point set* $\mathscr{A}$.

(d) *Point set* $\mathscr{B}$.

FIG. 3. *Locating the point sources with* 8 *directions and* 10% *noise.*

TABLE 4

Reconstruction of scattering strengths using the far fields with 10% *noise. We take* $\hat{x} = (\cos(\pi/16), \sin(\pi/16))$ *in this example.*

	True strength	Computed strength
τ_1	$0.119437 + 0.858134i$	$0.117949 + 0.860545i$
τ_2	$0.931100 + 0.056194i$	$0.939913 + 0.061328i$
τ_3	$0.994541 + 0.975031i$	$1.001599 + 0.981825i$
τ_4	$0.406819 + 0.595928i$	$0.405445 + 0.607381i$
τ_5	$0.117482 + 0.901291i$	$0.131289 + 0.911853i$

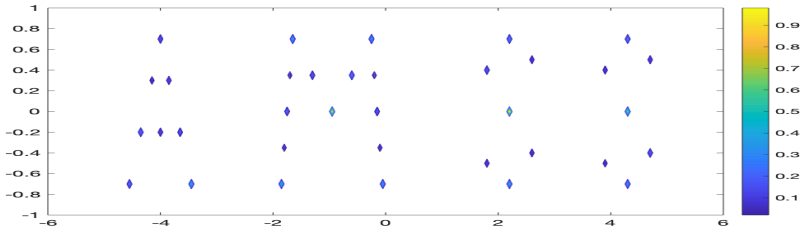

FIG. 4. *Reconstruction of "AMSS" with* 32 *directions and* 10% *noise.*

5.3. Small inclusions. In this part, we consider the reconstruction of small inclusions using the indicator (4.9). Two sound soft circles with radius 0.02 are located at $(0.5, 0.5)$ and $(1, 1)$, respectively. We take $k_- = 40$, $k_+ = 200$, $dk = 1$, and 10% relative noise in the numerical results. Sampling space 0.01 is used. Figure 5 gives the results using different numbers of observation directions.

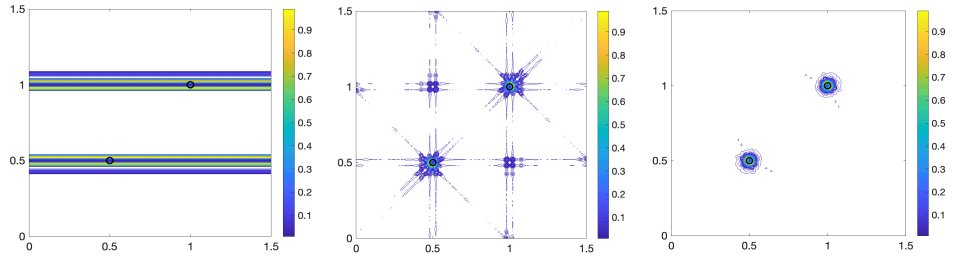

(a) 2 directions. (b) 8 directions. (c) 32 directions.

FIG. 5. *Locating the small circles by the backscattering far fields with* 10% *noise.*

6. Conclusions and remarks. We consider the determination of both the locations and the scattering strengths of point objects from multifrequency sparse data. Uniqueness results are proven for these inverse problems, and the involved formulas are used to develop computational methods. The proposed direct methods for locating the positions and recovering the scattering strengths are simple and fast. Some numerical examples further verify the accuracy and robustness of these methods in the presence of noise.

As shown in Figure 5, the location determination algorithm also works for small inclusions. This is due to the fact that the point objects can be regarded as an approximation of small inclusions.

REFERENCES

[1] A. Alzaalig, G. Hu, X. Liu, and J. Sun, *Fast acoustic source imaging using multi-frequency sparse data*, Inverse Problems, 36 (2020), 025009.

[2] H. Ammari and H. Kang, *Reconstruction of Small Inhomogeneities from Boundary Measurements*, Lecture Notes in Math. 1846, Springer-Verlag, Berlin, 2004.

[3] D. Colton and R. Kress, *Inverse Acoustic and Electromagnetic Scattering Theory*, 3rd ed., Springer, Berlin, 2013.

[4] A. J. Devaney, *Super-resolution Processing of Multi-static Data Using Time Reversal and MUSIC*, manuscript, 2000.

[5] L. L. Foldy, *The multiple scattering of waves.* I. *General theory of isotropic scattering by randomly distributed scatterers*, Phys. Rev., 67 (1945), pp. 107–119.

[6] R. Griesmaier and C. Schmiedecke, *A multifrequency MUSIC algorithm for locating small inhomogeneities in inverse scattering*, Inverse Problems, 33 (2017), 035015.

[7] R. Griesmaier and C. Schmiedecke, *A factorization method for multifrequency inverse source problems with sparse far field measurements*, SIAM J. Imaging Sci., 10 (2017), pp. 2119–2139, https://doi.org/10.1137/17M111290X.

[8] X. Ji and X. Liu, *Inverse Acoustic Scattering Problems with Multi-frequency Sparse Backscattering Far Field Data*, preprint, https://arxiv.org/abs/1906.02008, 2019.

[9] X. Ji and X. Liu, *Inverse elastic scattering problems with phaseless far field data*, Inverse Problems, 35 (2019), 114004.

[10] X. Ji and X. Liu, *Inverse electromagnetic source scattering problems with multifrequency sparse phased and phaseless far field data*, SIAM J. Sci. Comput., 41 (2019), pp. B1368–B1388, https://doi.org/10.1137/19M1256518.

[11] X. Ji, X. Liu, and B. Zhang, *Phaseless inverse source scattering problem: Phase retrieval, uniqueness and direct sampling methods*, J. Comput. Phys. X, 1 (2019), 100003.

[12] A. Kirsch, *The MUSIC algorithm and the factorization method in inverse scattering theory for inhomogeneous media*, Inverse Problems, 18 (2002), pp. 1025–1040.

[13] J. Sylvester and J. Kelly, *A scattering support for broadband sparse far field measurements*, Inverse Problems, 21 (2005), pp. 759–771.

[14] D. Zhang, Y. Guo, J. Li, and H. Liu, *Locating multiple multipolar acoustic sources using the direct sampling method*, Commun. Comput. Phys., 25 (2019), pp. 1328–1356.